

Oxidative Stress Contributes to Arsenic-induced Telomere Attrition, Chromosome Instability, and Apoptosis*

Received for publication, April 5, 2003, and in revised form, May 20, 2003
Published, JBC Papers in Press, May 26, 2003, DOI 10.1074/jbc.M303553200

Lin Liu^{‡§}, James R. Trimarchi^{‡§}, Paula Navarro[‡], Maria A. Blasco[¶], and David L. Keefe^{‡§||}

From the [‡]Department of Obstetrics and Gynecology, Women and Infants Hospital, Brown University, Providence, Rhode Island 02905, [§]Marine Biological Laboratory, Woods Hole, Massachusetts 02543, and [¶]Department of Immunology and Oncology, National Centre of Biotechnology, Madrid, E-28049, Spain

The environmental contaminant arsenic causes cancer, developmental retardation, and other degenerative diseases and, thus, is a serious health concern worldwide. Paradoxically, arsenic also may serve as an anti-tumor therapy, although the mechanisms of its antineoplastic effects remain unclear. Arsenic exerts its toxicity in part by generating reactive oxygen species. We show that arsenic-induced oxidative stress promotes telomere attrition, chromosome end-to-end fusions, and apoptotic cell death. An antioxidant, *N*-acetylcysteine, effectively prevents arsenic-induced oxidative stress, telomere erosion, chromosome instability, and apoptosis, suggesting that increasing the intracellular antioxidant level may have preventive or therapeutic effects in arsenic-induced chromosome instability and genotoxicity. Embryos with shortened telomeres from late generation telomerase-deficient mice exhibit increased sensitivity to arsenic-induced oxidative damage, suggesting that telomere attrition mediates arsenic-induced apoptosis. Unexpectedly, arsenite did not cause chromosome end-to-end fusions in telomerase RNA knockout mouse embryos despite progressively damaged telomeres and disrupting embryo viability. Together, these findings may explain why arsenic can initiate oxidative stress and telomere erosion, leading to apoptosis and anti-tumor therapy on the one hand and chromosome instability and carcinogenesis on the other.

Arsenic is a significant environmental concern worldwide because millions of people are at risk of drinking water contaminated by arsenic (1, 2). Epidemiological data show that chronic exposure of humans to inorganic arsenic is associated with hepatic injury, peripheral neuropathy, and increased rates of a wide variety of cancers, particularly of the skin, lung, bladder, and liver (3–5). Arsenic also produces toxic effects on the female reproductive system, including ovarian dysfunction (6), aberrant embryo development and lethality (7, 8), and postnatal growth retardation (9). Interestingly, it also has proven useful for anti-cancer therapy (10–12), although the mechanisms underlying its paradoxical (antineoplastic) effects remain unclear.

* This work was supported by Women and Infants Hospital/Brown Faculty Research Fund (to D. L. K.) and by grants from the Ministry of Science and Technology, Spain, and the European Union (to M. A. B.). The costs of publication of this article were defrayed in part by the payment of page charges. This article must therefore be hereby marked "advertisement" in accordance with 18 U.S.C. Section 1734 solely to indicate this fact.

|| To whom correspondence should be addressed: Laboratory for Reproductive Medicine, Marine Biological Laboratory, Woods Hole, MA 02543. Tel.: 508-289-7649; Fax: 508-540-6902; E-mail: dkeefe@wihri.org.

Many possible modes of arsenic action have been proposed, including chromosomal abnormalities, oxidative stress, altered DNA repair and DNA methylation patterns, altered cell proliferation, abnormal gene amplification, and inhibition of p53 and telomerase (5, 13–18). In particular, arsenic exerts its toxicity by generating reactive oxygen species (ROS)¹ (19–22). Mitochondria, the main source of ROS production, which also play a crucial role in the control of apoptosis (23, 24), have been implicated in arsenite-induced apoptosis (21, 25). Thus, mitochondrial dysfunction may explain the cytotoxicity and degenerative effects induced by arsenic. How ROS links arsenic exposure to carcinogenesis is still not well understood.

Vertebrate telomeres consist of tandem repeats of G-rich sequence that cap the ends of chromosomes, protecting them from fusion and chromosomal instability. The telomerase RNA template (TR) cooperates with telomerase reverse transcriptase, the catalytic subunit, to form active telomerase, which is primarily responsible for telomere elongation during cell division (26). Telomere shortening, chromosome end-to-end fusion, and reactivation of telomerase are known to promote carcinogenesis in p53 mutant backgrounds (27–29). Human cells are more sensitive to arsenite than are cells of rodent origin (30, 31), and one possible reason for this difference could be attributed to the short telomeres found in human cells (32–34). Differences between mouse and human telomeres limit the laboratory mouse as a straightforward model to critically test the role of telomere dysfunction and telomerase in human malignancy (35). However, telomerase RNA knockout (TR^{-/-}) mice show progressive telomere shortening and chromosome instability with increasing generations and also exhibit defects in highly proliferative tissues, affecting fetal development, growth, immune function, and carcinogenesis (36–40). ROS can damage telomeres and lead to genomic instability (41). We sought to investigate the influence of arsenic on both mitochondrial function and genomic instability using mouse early embryos as models. This experimental model has a unique advantage such that it allows non-invasive assessment of cell viability by direct observation of cleavage and blastocyst formation as well as precise control over confounding variables possibly present in intact animal models. We further examined whether TR^{-/-} mice, with shortened telomeres, are more sensitive to arsenite-induced genotoxicity, similar to human cells.

We show that arsenic-induced oxidative stress promotes telomere attrition, chromosome end-to-end fusions, and apoptotic cell death. An antioxidant, *N*-acetylcysteine, effectively prevents arsenic-induced oxidative stress, telomere erosion, chro-

¹ The abbreviations used are: ROS, reactive oxygen species; TR^{-/-}, telomerase knockout; WT, wild type; NAC, *N*-acetylcysteine; TMRE, tetramethylrhodamine ethyl ester; FISH, fluorescence *in situ* hybridization.

mosome instability, and apoptosis, further supporting the notion that oxidative stress is involved in arsenic-induced chromosome instability and genotoxicity.

EXPERIMENTAL PROCEDURES

Mice, Embryos, and in Vitro Culture—Outbred CD1 mice or telomerase-deficient mice (36) were used in this experiment. Female mice were induced to super-ovulate by consecutive injection of pregnant mare's serum gonadotropin and human chorionic gonadotropin and mated with proven fertile males. Zygotes were collected from oviducts 20–21 h after injection of human chorionic gonadotropin and cultured at 37 °C in a humidified atmosphere of 7% CO₂ in potassium simplex optimized media supplemented with nonessential amino acids (42).

Measurement of Mitochondrial Membrane Potential and Reactive Oxygen Species—Dynamics in the mitochondrial membrane potential ($\Delta\psi_m$) were measured by quantification of fluorescence intensity of cells stained with the probe tetramethylrhodamine ethyl ester (TMRE) (Molecular Probes, Eugene, OR). Zygotes were loaded with 150 nM TMRE in potassium simplex optimized media for 30 min at 37 °C, and relative TMRE fluorescence intensity was imaged in HEPES-buffered potassium simplex optimized media containing 50 nM TMRE using an epifluorescence microscope (Zeiss) and analyzed using MetaMorph imaging software (Universal Imaging Corporation, Downingtown, PA). Fluorescence was acquired at the excitation wavelength of 530 nm and emission wavelength of 580 nm. The intracellular production of ROS was determined using the fluorescent probe carboxymethyl dichlorofluorescein diacetate (Molecular Probes). Zygotes were loaded with 5 μ M carboxymethyl dichlorofluorescein diacetate at 37 °C for 25 min and washed, and carboxymethyl dichlorofluorescein fluorescence was measured at an excitation wavelength of 488 nm and an emission wavelength of 520 nm.

Immunocytochemistry for Localization of Cytochrome *c*—Release of cytochrome *c* from mitochondria was assessed by immunocytochemistry (43). Embryos were fixed in 4% paraformaldehyde, washed, and incubated with a mouse monoclonal anti-cytochrome *c* antibody (Pharmin-gen). Embryos were washed and then incubated with Texas Red anti-mouse IgG secondary antibody (Vector Laboratories, Burlingame, CA). Cytochrome *c* localization was detected by fluorescence microscopy using a Texas Red filter (excitation 595 nm, emission 610–615 nm).

Detection of Telomere Length Using Quantitative Fluorescence in Situ Hybridization (FISH) with a Telomere Probe—Embryos were arrested at metaphase with nocodazole (0.5 μ g/ml) and prepared for chromosome spreads. FISH with fluorescein isothiocyanate-labeled (CCCTAA)₃ peptide nucleic acid probe (Applied Biosystems, Framingham, MA) was performed according to the manufacturer's protocol. Chromosomes were counterstained with 0.2 μ g/ml Hoechst 33342. Embryos were mounted onto a glass slide in Vectashield mounting medium (Vector Laboratories). Telomeres were detected using a fluorescein isothiocyanate filter with a Zeiss fluorescence microscope (Axiophot), and images were captured by an AxioCam and AxioVision 3.0 software. Telomere detection using peptide nucleic acid probe for mouse cells has been described previously (34).

Apoptotic Assay—DNA fragmentation was detected by the TdT-mediated dUTP nick-end labeling assay using the *in situ* cell death detection kit (Roche Diagnostics) according to manufacturer's instruction, and nuclei were counterstained with 50 μ g/ml propidium iodide (Molecular Probes) and assessed by a Zeiss fluorescence microscopy. Statistical significance was analyzed by analysis of variance using StatView software (SAS, Cary, NC).

RESULTS

Arsenite Compromises Embryo Viability—Survival of outbred CD-1 mouse embryos was compromised by exposure to arsenite in a time- and dose-dependent manner (Fig. 1). Embryo viability, determined by both cleavage at 20–24 h and the ability to develop to the blastocyst stage at 90–96 h in culture (Fig. 1A), was not affected by exposure to 2 μ g/ml arsenite for 2 h. The dosage was chosen based on previous study using sodium arsenite (20, 22). However, exposure of zygotes to 2 μ g/ml arsenite overnight (20 h) completely inhibited cleavage and subsequent development in all embryos ($n = 44$). Increasing doses of arsenite over a 2-h exposure progressively reduced embryo survival (Fig. 1B). Exposure of mouse zygotes to 4 or 8 μ g/ml arsenite significantly reduced cleavage rate (78%, $n = 64$

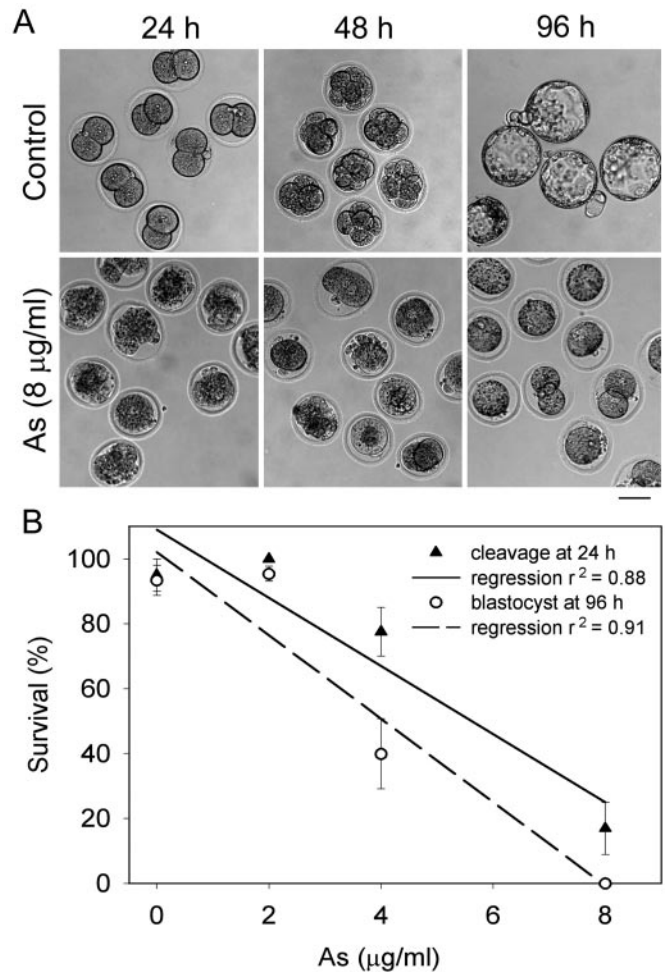


FIG. 1. Arsenite inhibits survival of CD1 mouse embryos in a dose-dependent manner. A, untreated normal zygotes as controls cleaved to 2 cells at 20–24 h, 4–8 cells at 48 h, and blastocysts at 90–96 h in culture, whereas zygotes treated with 8 μ g/ml sodium arsenite (As) for 2 h exhibited blebbing, cell shrinkage at 20–24 h, apoptotic fragmentation at 48 h, and cell death at 96 h, with very few cleaved to 2 cells. Bar, 50 μ m. B, survival curve for CD1 mouse embryos exposed to increased doses of sodium arsenite for 2 h. Each data point (mean \pm S.E.) represents an average of four experiments.

or 17%, $n = 67$, respectively) compared with control zygotes (95%, $n = 72$, $p < 0.01$). By 90–96 h, most (93%) untreated embryos reached the blastocyst stage, whereas only 40% of zygotes treated with 4 μ g/ml arsenite and none of zygotes treated with 8 μ g/ml arsenite reached blastocyst stage.

The total cell number in blastocysts derived from zygotes treated with 4 μ g/ml arsenite for 2 h was significantly reduced, and apoptosis was significantly increased (37 ± 12.5 and 6.0 ± 2.2 , respectively, $n = 7$) compared with those of controls (52.5 ± 15.4 and 2.5 ± 2.1 , respectively, $n = 11$; $p < 0.01$) (Fig. 2A and B, and D and E). The total cell number in developed blastocysts did not differ between zygotes treated with 2 μ g/ml arsenite and untreated zygotes as control (Fig. 2, D and E). Many of the arrested embryos that failed to reach blastocysts showed apoptotic cell death (Fig. 2C). These results demonstrate that arsenite affects embryo viability through apoptosis.

Arsenite Causes Mitochondrial Dysfunction and Promotes ROS Production—To further determine mechanisms of arsenic-induced apoptosis and inhibition of cell survival, we examined mitochondrial membrane potential, ROS, and cytochrome *c* release, an early signal of apoptosis. Arsenite gradually disrupted the mitochondrial membrane potential ($\Delta\psi_m$) (Fig. 3A). Adding vehicle did not change $\Delta\psi_m$ in controls. At 60 min after

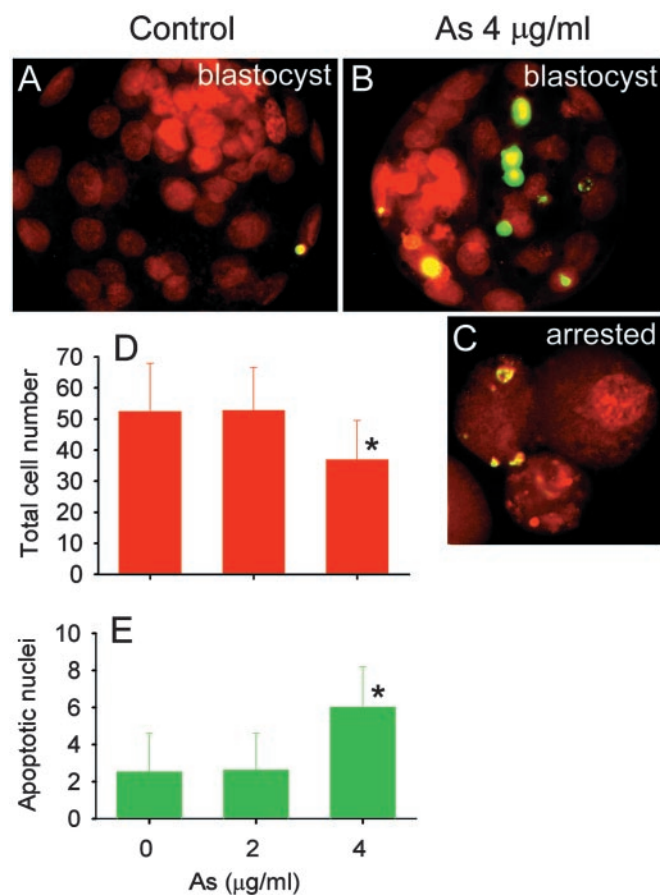


FIG. 2. Apoptosis is increased in arsenite-treated embryos. *A*, control blastocyst showed total cell nuclei stained by propidium iodide (red) and one apoptotic nucleus (yellow green). *B*, a blastocyst (*B*) and arrested embryos (*C*) derived from zygotes treated with 4 μg/ml arsenite for 2 h showed increased apoptotic nuclei and fewer cells. *D*, total cell number (mean ± S.D.) is significantly less. *E*, apoptotic cell number (mean ± S.D.) is significantly increased ($p < 0.01$) in blastocysts from 4 μg/ml arsenite-treated zygotes than non-treated and 2 μg/ml arsenite-treated zygotes.

exposure to 8 μg/ml arsenite, the $\Delta\psi_m$ was significantly reduced compared with that of controls (62.4 ± 12.1 and $87.2 \pm 3.8\%$, respectively, $n = 5$, $p < 0.001$). From 80 min after exposure to arsenite, the $\Delta\psi_m$ reduced to half the levels of normal controls. Zygotes treated with 8 μg/ml arsenite exhibited obvious membrane blebbing and cell shrinkage 24 h after treatment followed by cytofragmentation at 48 h (Fig. 1A). These morphological events are consistent with apoptosis induced by acute oxidative stress. Embryos treated with 8 μg/ml for 1 h cleaved normally to equal 2 cells and developed further to blastocysts, indicating that mitochondrial dysfunction occurs before developmental impairment.

ROS were significantly increased after exposure of zygotes to arsenite (8 μg/ml) for 2 h compared with controls (relative fluorescence intensity valued at 2.1 ± 0.31 , $n = 11$, and 1.0 ± 0.09 , $n = 10$, respectively, Fig. 3B). The increased ROS production coincided with sustained low $\Delta\psi_m$ after arsenite challenge. At 2 h after exposure of zygotes to 8 μg/ml arsenite, cytochrome *c* was localized in mitochondria and was not abnormally distributed compared with control zygotes, which displayed reticulate and punctate staining, indicative of localization of mitochondria (43) (data not shown) (Fig. 3C). However, zygotes treated with 8 μg/ml arsenite for 2 h, then washed and cultured in normal medium for a further 5 h exhibited a diffuse distribution of cytochrome *c* staining in the cytoplasm, indicative of its release from mitochondria into cytoplasm. These results

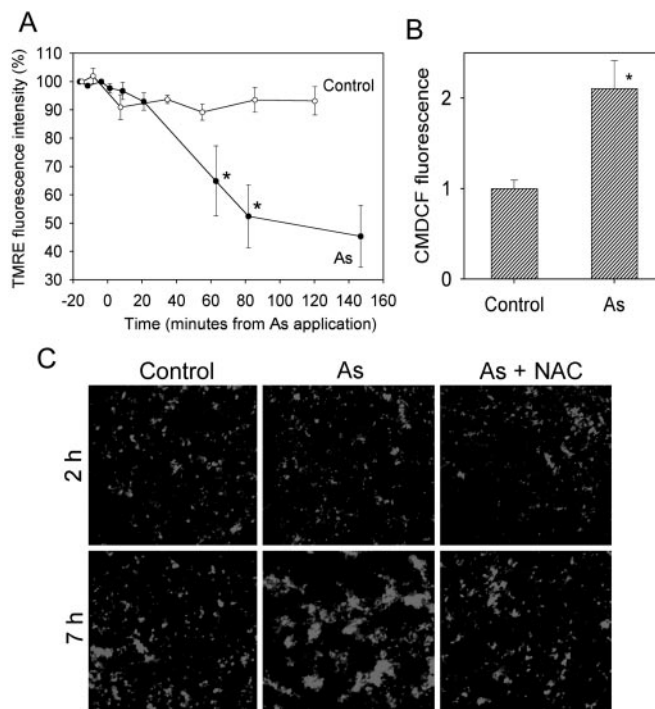


FIG. 3. Arsenite induces mitochondrial dysfunction and oxidative stress. Zygotes treated with 8 μg/ml arsenite exhibited significantly decreased mitochondrial membrane potential measured by TMRE fluorescence intensity (mean ± S.D.) 60 min after treatment (*A*) and significantly increased reactive oxygen species, indicated by carboxymethyl dichlorofluorescein fluorescence 2 h after treatment (*B*), and the release of cytochrome *c* from mitochondria, as indicated by diffuse cytochrome *c* staining in the cytoplasm 7 h after treatment. Control embryos showed punctate staining of cytochrome *c* in the mitochondria (*C*). The asterisk indicates $p < 0.01$, compared with controls.

show that oxidative stress and apoptosis links arsenic actions to mitochondrial dysfunction.

Antioxidant Rescues Embryos from Arsenite Toxicity—If arsenic-induced ROS caused cell death, then adding antioxidants might prevent embryos from undergoing apoptosis, and promoted cell survival. The antioxidant, *N*-acetylcysteine (NAC), which scavenges ROS, at a concentration of 30 mM effectively prevented cytochrome *c* release from mitochondria in zygotes challenged by arsenite (Fig. 3C). Arsenite-treated embryos consistently manifested membrane blebbing with no cleavage at 20–24 h and no blastocyst formation at 90–96 h (Fig. 4, *A* and *B*). Not unexpectedly, NAC rescued embryos from blebbing and promoted development to blastocysts. Zygotes co-treated with NAC and arsenite cleaved and developed to blastocysts at a frequency significantly ($p < 0.01$) higher than that of zygotes treated with only 2 μg/ml arsenite for 20 h or 4 or 8 μg/ml arsenite for 2 h but were indistinguishable from those of NAC-treated embryos as control (Fig. 4C). A majority of blastocysts from embryos co-treated with arsenite and NAC were expanded or hatching, but the few blastocysts that survived from arsenite treatment without NAC were not expanded or hatching. The total cell number and apoptotic cells did not differ between blastocysts that developed from zygotes co-treated with NAC and arsenite and NAC controls ($p > 0.05$, Fig. 4D). Thus, antioxidant prevents oxidative stress induced by arsenite and increases cell survival.

Oxidative Stress by Arsenite Causes Telomere Dysfunction and Genomic Instability—We and others previously showed that oxidative stress could damage telomeres. We further tested whether telomere shortening and chromosome fusion underlies arsenite-induced oxidative stress and cell death. It has been shown that the shortest telomeres, as evidenced by

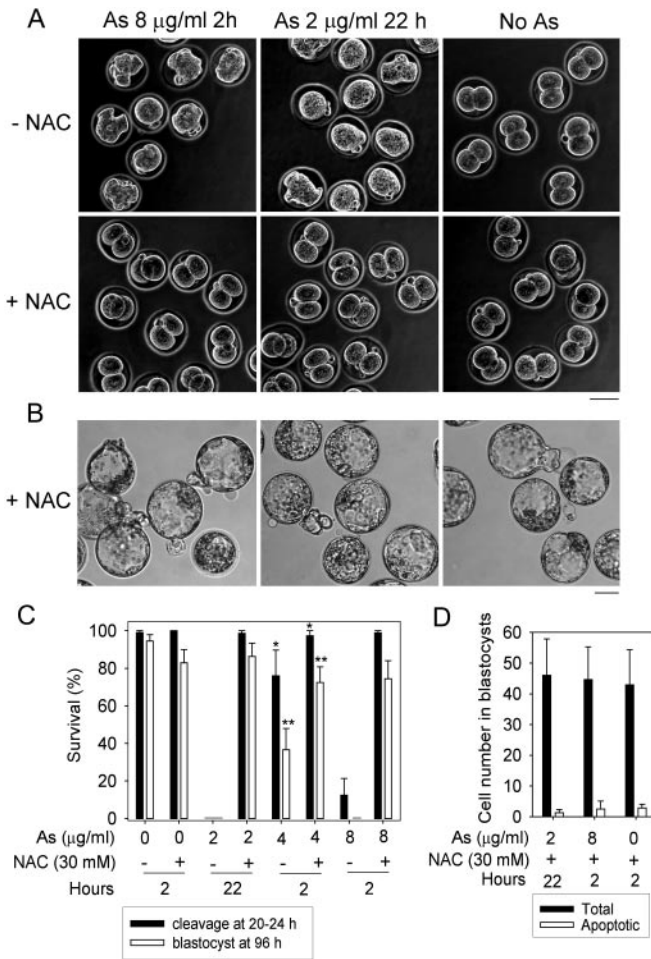


FIG. 4. Antioxidant protects embryos from arsenite-induced oxidative damage. Representative images showing zygotes co-treated with arsenite and antioxidant NAC (30 mM) cleaved normally to 2-cell stage at 20–24 h (A) and blastocysts at 90–96 h (B). C, 30 mM NAC effectively rescued embryo survival, indicated by rates (mean ± S.E., 3–4 replicates) of cleavage and blastocyst formation regardless of arsenite treatment at 4 or 8 μg/ml for 2 h or 2 μg/ml for 22 h. The single asterisk (*) and double asterisks (**) indicate $p < 0.01$ for cleavage and blastocyst, respectively. D, the total cell number and apoptotic cells did not differ (mean ± S.D., $p > 0.05$) in blastocysts from zygotes co-treated by arsenite and NAC, compared with those of NAC controls.

invisible telomere fluorescence signals evaluated with quantitative FISH, trigger chromosome end-to-end fusions and impair cell viability (44, 45). We also utilized the absence of obvious telomere fluorescence signals at the end of chromosomes and chromosome fusion by quantitative FISH to indicate telomere dysfunction as well as chromosome instability. Chromosome spreads of normal blastocysts from untreated CD-1 mouse zygotes ($n = 40$) showed obvious telomere fluorescence signals at each chromosome end and normal chromosomal ploidy (Fig. 5A). No obvious telomere loss or chromosome fusions were found. Higher doses of arsenite (8 μg/ml) caused embryos to arrest at interphase or undergo apoptosis, with no chromosome spreads suitable for telomere analysis. Some zygotes exposed to 4 μg/ml arsenite for 2 h, which had arrested at interphase stage from 2-cell stage to morula stage, also failed to produce mitotic chromosome spreads, preventing analysis for telomere function. However, 43% of arrested embryos ($n = 14$) with observable chromosome spreads harbored either at least one chromosome end-to-end fusion where telomere signals were not readily visible (Fig. 5, B and C) or fragmented chromosomes with extensive erosion of telomere signals. Thirty percent of surviving blastocysts ($n = 20$) also showed one or

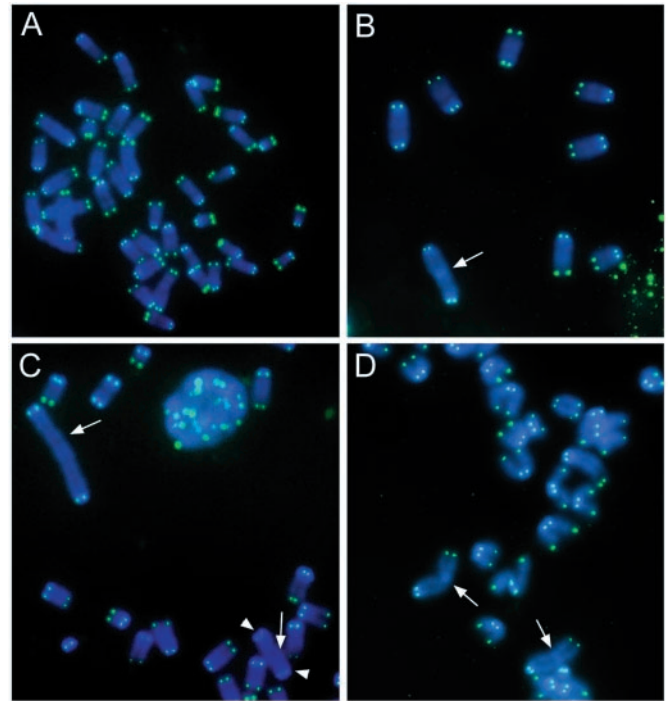


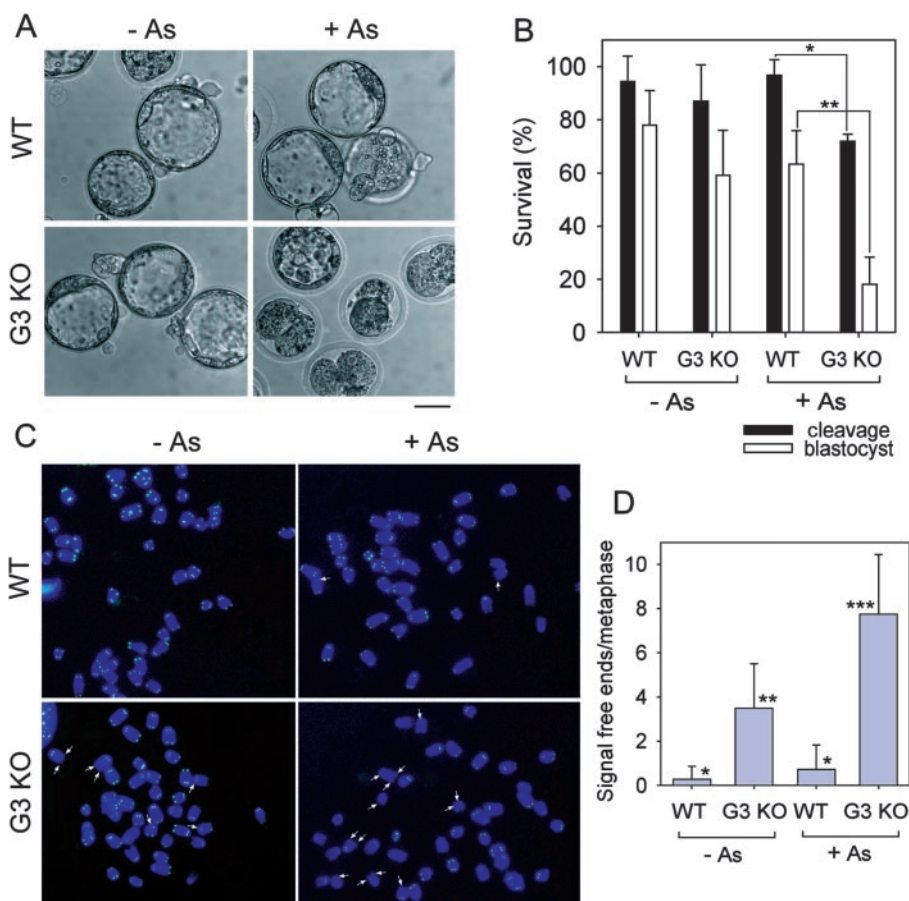
FIG. 5. Arsenite damages telomeres and causes chromosome end-to-end fusion in CD1 mouse embryos. A, a normal chromosome spread from untreated blastocysts showing telomere fluorescence signals at the ends of chromosomes. B–D, arsenite (4 μg/ml) induced loss of telomere fluorescence signals at the chromosome ends where chromosomes are fused (arrows) in arrested embryos (B and C) and a survived blastocyst (D). Arrowheads indicate two centromere regions at the p-arm. Telomeres (green) are detected by peptide nucleic acid telomere probe using FISH. Chromosomes (blue) were counter-stained by DNA dye Hoechst 33342.

more telomere losses and chromosome end-to-end fusions (Fig. 5D). Chromosome end-to-end fusions were found more frequently at the p-arm close to centromeres, brightly stained by DNA dye Hoechst or 4,6-diamidino-2-phenylindole (Fig. 5, B and D), than at the q-arm of chromosomes (Fig. 5C). Aneuploidy was consistently observed in embryos with telomere loss and chromosome fusions.

If the observed telomere dysfunction and chromosome end-to-end fusions were indeed triggered by ROS produced by arsenite-stressed mitochondria, then reducing ROS with an antioxidant would expectedly prevent telomere loss and chromosome fusions. Indeed, co-treatment of arsenite and NAC significantly reduced telomere dysfunction and chromosome fusion. In 50 chromosome spreads analyzed, only 3 (6%) from arrested embryos showed telomere loss and chromosome end-to-end fusion, indicating that embryos failed from rescue by antioxidants exhibited similar phenotypes of embryos treated with arsenite alone. Other chromosome spreads showed obvious telomere signals at the chromosome ends and normal ploidy. Again, these results suggest that maintenance of telomere function in chromosomes and therein of embryo viability by oxidant scavenger NAC may be a consequence of embryos having escaped from the significantly reduced oxidative stress. Thus, ROS could be an important mediator that links arsenite toxicity, mitochondrial dysfunction, telomere shortening and erosion, genomic instability, and cell viability.

Telomerase-deficient Mouse Embryos with Shortened Telomeres Are More Sensitive to Arsenite-mediated Inhibition of Cell Survival—To further confirm that arsenic-induced oxidative stress and increased apoptosis resulted from telomere dysfunction, we compared embryo survival after exposure to arsenic treatment between wild-type (WT) and age-matched,

FIG. 6. Late generation telomerase knockout ($TR^{-/-}$) mouse (G3 KO) embryos manifest increased susceptibility to arsenite-induced oxidative damage. *A*, very few unexpanded blastocysts at 96 h after treatment were derived from G3 KO embryos treated with 4 μ g/ml arsenite, compared with WT controls. *B*, rates of cleavage and blastocyst formation are significantly less in G3 KO embryos than in WT embryos (mean \pm S.D.; * $p = 0.0284$, ** $p < 0.01$). *C*, telomere FISH images of G3 KO mouse embryos showing telomere attrition (arrows) and arsenite (4 μ g/ml) induced severe absence of visible telomere fluorescence signals. Note: no chromosome end-to-end fusions are found. Green, telomeres; blue, chromosomes. *D*, telomere fluorescence signal free ends/metaphase chromosome is significantly increased in G3 KO embryos and in G3 KO embryos treated with arsenite (4 μ g/ml). *, $p < 0.0284$; **, $p < 0.01$, ***, $p < 0.0001$.



third generation telomerase-deficient mice (G3 $TR^{-/-}$) with shortened telomeres (36, 37, 42). Young G3 $TR^{-/-}$ mice were chosen because cells from these mice show no chromosome fusions with relatively shortened telomeres compared with wild-type cells (40, 44). G3 $TR^{-/-}$ zygotes treated with 4 μ g/ml arsenite cleaved at a significantly lower rate than WT zygotes treated with the same concentration of arsenite (97.0 ± 5.8 and $71.9 \pm 2.7\%$, respectively, $p = 0.0284$). Furthermore, G3 $TR^{-/-}$ zygotes treated with arsenite developed to blastocysts at a considerably lower incidence compared with those of G3 $TR^{-/-}$ zygotes without arsenite treatment and of WT zygotes treated with or without 4 μ g/ml arsenite (18 versus 59–78%, $p < 0.001$) (Fig. 6, A and B). In addition, expanded blastocysts, indicative of viable embryos, were found in WT zygotes treated with or without 4 μ g/ml arsenite and G3 $TR^{-/-}$ zygotes without arsenite treatment but not from G3 $TR^{-/-}$ zygotes treated with arsenite. Rates of cleavage (87–97%) did not differ between WT zygotes treated with or without 4 μ g/ml arsenite and G3 $TR^{-/-}$ zygotes without arsenite treatment. Both WT zygotes treated with arsenite and G3 $TR^{-/-}$ zygotes with no arsenite treatment exhibited decreased rates of blastocyst formation (63.3 ± 12.6 and $59.1 \pm 17.1\%$, respectively) compared with non-treated WT zygotes ($78 \pm 13.1\%$, $n = 35$ –40). Many G3 $TR^{-/-}$ fertilized eggs showing only one or no pronucleus were discarded, since they indicated aberrant fertilization, which itself would have affected cleavage and early development, as we recently reported (42). These results unambiguously demonstrate that telomerase-deficient mouse embryos with shortened telomeres are more sensitive than wild-type embryos to arsenic-mediated inhibition of cell survival. This is in agreement with previous observations that telomerase inhibition in human cells with short telomeres damages chromosomes and triggers apoptosis (46, 47).

We compared telomere signals in WT and G3 $TR^{-/-}$ embryos after treatment with or without 4 μ g/ml arsenite. Treated WT embryos showed telomere fluorescence signals at the ends of chromosomes, with only 0.7 ± 1.1 telomere signal-free ends/metaphase ($n = 25$), which was not different from that of untreated WT embryos (0.3 ± 0.6 , $n = 15$) (Fig. 6, C and D). By contrast, the incidence of telomere signal-free ends/metaphase was significantly higher in G3 $TR^{-/-}$ embryos with no arsenite treatment and even further increased in G3 $TR^{-/-}$ embryos treated with arsenite (3.5 ± 2.0 , $n = 28$, and 7.8 ± 2.7 , $n = 20$, respectively, $p < 0.001$), suggesting that G3 $TR^{-/-}$ embryos with shortened telomeres were more susceptible to arsenite-induced oxidative damage. One (13%) of eight arrested embryos with chromosome spreads of WT zygotes treated with arsenite showed one chromosome end-end fusion where telomere signals were invisible. Surprisingly, chromosome end-to-end fusions were not found in spreads available for analysis of telomerase-deficient mouse embryos, even with significantly shortened or absent telomeres, in contrast to the observation in CD-1 mouse embryos. Although the mechanisms underlying this difference have not been elucidated, we speculate that telomerase RNA may be involved in modulating the chromosome sensitivity to telomere loss. Acute treatment with arsenic combined with inhibitors directed at the RNA component of telomerase (e.g. RNA-mediated interference) might provide an effective strategy to block tumorigenesis, as suggested for anti-tumor drugs using telomerase inhibitors (48).

DISCUSSION

We show that arsenite disrupts mitochondrial function and induces oxidative stress, leading to telomere attrition, chromosome end-to-end fusions, and decreased embryo viability. We also demonstrate that the antioxidant NAC protects embryos

stressed by arsenite against telomere attrition, chromosome instability, and cell death. Furthermore, telomerase-deficient mouse embryos with significant telomere shortening exhibit enhanced susceptibility to arsenite-induced oxidative damage compared with age-matched, wild-type embryos. All these lines of evidence suggest that oxidative stress resulting from exposure to arsenite leads to telomere attrition and dysfunction and chromosome instability and disrupts embryo viability through a mechanism of apoptosis.

Although it is also possible that inhibition of telomerase by arsenic may cause telomere attrition and chromosome fusion (18), in our study significant loss of telomeres occurred within 72–96 h after application of medium doses of arsenite, when cell replications were limited. Normally, numerous cell doublings are required for telomere attrition without telomerase. It is likely that oxidative stress induced by arsenic directly damages telomeres and causes genomic instability and/or apoptosis. Indeed, direct administration of oxidants to cells damages DNA, breaks polyguanosine sequences in telomere repeats, and causes telomere shortening, cell cycle arrest, and replicative senescence (49, 50). Oxidative stress links mitochondrial dysfunction and telomere attrition and genomic instability (41). Together, we suggest that oxidative stress produced by arsenite directly erodes telomere sequences, leading to telomere dysfunction and genomic instability.

It has been demonstrated that the chromosome with the shortest telomere is the most unstable and most likely to fuse with another chromosome with a short telomere (44). Medium dose (4 $\mu\text{g}/\text{ml}$) arsenite induced oxidative stress, telomere attrition, and chromosome end-to-end fusions in CD-1 mouse embryos. Unexpectedly, in telomerase RNA knockout mouse embryos this dose of arsenite did not cause chromosome end-to-end fusions, although arsenite induced oxidative stress-eroded telomeres at the end of chromosomes and impaired embryo viability. The underlying mechanism is not yet clear at this point. Interestingly, a recent finding shows that telomerase RNA is elevated in the presence of arsenic, coincident with the appearance of chromosome end-to-end fusions (18). Together, these findings suggest an important role for wild-type telomerase RNA in mediating chromosome end-to-end fusion at the stage of critically shortened or absent telomeres. Arsenite combined with inhibitors directed at the RNA component of telomerase (*e.g.* RNA-mediated interference) might provide an effective strategy to block chromosome fusion and, thus, tumorigenesis in some circumstances.

Arsenic-induced telomere oxidation may explain the dual role of arsenic in tumorigenesis and anti-tumor therapy. Coincidentally, telomeres also play a dual role in tumorigenesis and replicative senescence. Chromosome end-to-end fusions and chromosome instability do not necessarily lead to inhibition of cell viability and cell death but are known to be critical initiators of carcinogenesis. Telomerase up-regulation takes place during the development of cancer after telomere shortening and chromosome instability (51–53). Indeed, telomerase knockout mice with shortened telomeres are resistant to tumor development in multistage skin carcinogenesis (29). This study suggests that short telomeres also could function as a tumor suppressor mechanism and that the absence of telomerase exerts a negative impact on papilloma formation. Nonetheless, late generation telomerase knockout old mice with shortened telomeres show an increased incidence of spontaneous malignancies, such as lymphoma, teratocarcinoma, and hepatoma (40). Such variable responses to telomere attrition are consistent with the notion that different cell types or ages may vary in their sensitivity to the chromosomal instability produced by telomere loss or to the activation of telomere rescue mecha-

nisms (29). Whether arsenite induces oxidative stress at a level that induces apoptosis or telomere attrition and chromosome instability also may depend on the status of other intracellular regulators, *e.g.* p53. Arsenite reduces p53 levels and disrupts the p53-mdm2 loop regulating cell cycle arrest, a suggestive model for arsenic-related skin carcinogenesis (5).

Doses of arsenite exposure certainly affect cell death and survival. For example, high dose (8 $\mu\text{g}/\text{ml}$) arsenite caused only cell arrest and death with no survival and a lack of metaphase chromosomes available for telomere and ploidy analysis. Mitochondria play a pivotal role in arsenite-induced toxicity, and arsenite disrupts mitochondrial membrane potential and increases ROS production, leading to cytochrome *c* release, a key component of early apoptosis. Cytochrome *c* release also may indicate dysfunction of mitochondria. Arsenite can induce apoptosis via a direct effect on the mitochondrial permeability transition pore (25). Oxidative stress often results from an imbalance between oxidants and antioxidants. NAC has been known to act as an antioxidant/free radical scavenger or reducing agent (54) that protects cells against cell death (55). Our results also demonstrate that increasing intracellular antioxidant levels may have preventive or therapeutic effects in arsenic-induced chromosome instability and genotoxicity. This evidence supports critical roles of mitochondria and ROS in arsenite-induced apoptosis (20, 21, 25, 56). The decreased cell viability and increased apoptosis may be utilized for anti-cancer therapy. Molecular studies and ongoing clinical trials suggest that as a chemotherapeutic agent arsenic trioxide shows great promise in the treatment of some malignancies (12, 57).

Using mouse early embryos as a model, we show that high dose (8 $\mu\text{g}/\text{ml}$) arsenite induced apoptosis in a typical mitochondrial-dependent pathway. Lower doses of arsenite resulted in chromosome end-to-end fusions with loss of telomeres. We propose that mild or chronic exposure to arsenite, mimicking circumstances of environmental contamination, gradually erodes telomeres, preferentially resulting in chromosome fusion and instability and initiating carcinogenesis, whereas exposure to acute high dose arsenite preferentially leads to rapid apoptosis, useful for anti-tumor therapy. In addition, early mouse embryos can be useful as a potential bioassay for toxicant and drug testing.

Although the present work produced interesting insights into mechanisms of arsenic effects using the mouse embryo model, human responses to arsenic may vary depending on exposure time and dosage, genetic background, and cell types, etc. Environmental contamination of arsenic can be acute and severe in some places but more chronological in others. In certain parts of Bangladesh and West Bengal, India, as many as 5% of sampled drinking wells have arsenic levels exceeding 1000 $\mu\text{g}/\text{liter}$, and 27% of wells have levels exceeding 300 $\mu\text{g}/\text{liter}$ (1), considerably higher than the current United States maximum contaminant level of 50 $\mu\text{g}/\text{liter}$. Although water supplies in the United States are generally low in arsenic, there have been reports of arsenic contamination of ground water in the Southwest, with levels in the hundreds and, in a few cases, more than 1000 $\mu\text{g}/\text{liter}$ (2). In addition, human cells have short telomeres, whereas mouse has ultra-long telomeres (32–34), which may contribute to increased susceptibility of human cells to arsenic toxicity compared with cells of rodent origin (30, 31). Although it is complicated to estimate daily consumption of arsenic by individuals in the contaminated areas and the quantity taken up by various types of cells, data obtained from our experiments using the mouse embryo model as well as from previous somatic cell models (20, 22) might be relevant to the public health problem with arsenic.

REFERENCES

1. Chappell, W. R., Beck, B. D., Brown, K. G., Chaney, R., Cothorn, R., Cothorn, C. R., Irgolic, K. J., North, D. W., Thornton, I., and Tsongas, T. A. (1997) *Environ. Health Perspect.* **105**, 1060–1067
2. Warner, M. L., Moore, L. E., Smith, M. T., Kalman, D. A., Fanning, E., and Smith, A. H. (1994) *Cancer Epidemiol. Biomark. Prev.* **3**, 583–590
3. Taylor, P. R., Qiao, Y. L., Schatzkin, A., Yao, S. X., Lubin, J., Mao, B. L., Rao, J. Y., McAdams, M., Xuan, X. Z., and Li, J. Y. (1989) *Br. J. Ind. Med.* **46**, 881–886
4. Leonard, A., and Lauwerys, R. R. (1980) *Mutat. Res.* **75**, 49–62
5. Hamadeh, H. K., Vargas, M., Lee, E., and Menzel, D. B. (1999) *Biochem. Biophys. Res. Commun.* **263**, 446–449
6. Chattopadhyay, S., Ghosh, S., Debnath, J., and Ghosh, D. (2001) *Arch. Environ. Contam. Toxicol.* **41**, 83–89
7. Muller, W. U., Streffer, C., and Fischer-Lahdo, C. (1986) *Arch. Toxicol.* **59**, 172–175
8. Tabocova, S., Hunter, E. S., III, and Gladen, B. C. (1996) *Toxicol. Appl. Pharmacol.* **138**, 298–307
9. Golub, M. S., Macintosh, M. S., and Baumrind, N. (1998) *J. Toxicol. Environ. Health B. Crit. Rev.* **1**, 199–241
10. Zhu, X. H., Shen, Y. L., Jing, Y. K., Cai, X., Jia, P. M., Huang, Y., Tang, W., Shi, G. Y., Sun, Y. P., Dai, J., Wang, Z. Y., Chen, S. J., Zhang, T. D., Waxman, S., Chen, Z., and Chen, G. Q. (1999) *J. Natl. Cancer Inst.* **91**, 772–778
11. Huan, S. Y., Yang, C. H., and Chen, Y. C. (2000) *Leuk. Lymphoma* **38**, 283–293
12. Zhu, J., Chen, Z., Lallemand-Breitenbach, V., and De The, H. (2002) *Nat. Rev. Cancer* **2**, 705–714
13. Kitchin, K. T. (2001) *Toxicol. Appl. Pharmacol.* **172**, 249–261
14. Goering, P. L., Aposhian, H. V., Mass, M. J., Cebrian, M., Beck, B. D., and Waalkes, M. P. (1999) *Toxicol. Sci.* **49**, 5–14
15. Gonsebatt, M. E., Vega, L., Salazar, A. M., Montero, R., Guzman, P., Blas, J., Del Razo, L. M., Garcia-Vargas, G., Albores, A., Cebrian, M. E., Kelsh, M., and Ostrosky-Wegman, P. (1997) *Mutat. Res.* **386**, 219–228
16. Barrett, J. C., Lamb, P. W., Wang, T. C., and Lee, T. C. (1989) *Biol. Trace Elem. Res.* **21**, 421–429
17. Nakamuro, K., and Sayato, Y. (1981) *Mutat. Res.* **88**, 73–80
18. Chou, W. C., Hawkins, A. L., Barrett, J. F., Griffin, C. A., and Dang, C. V. (2001) *J. Clin. Invest.* **108**, 1541–1547
19. Wang, T. S., and Huang, H. (1994) *Mutagenesis* **9**, 253–257
20. Hei, T. K., Liu, S. X., and Waldren, C. (1998) *Proc. Natl. Acad. Sci. U. S. A.* **95**, 8103–8107
21. Chen, Y. C., Lin-Shiau, S. Y., and Lin, J. K. (1998) *J. Cell. Physiol.* **177**, 324–333
22. Liu, S. X., Athar, M., Lippai, I., Waldren, C., and Hei, T. K. (2001) *Proc. Natl. Acad. Sci. U. S. A.* **98**, 1643–1648
23. Kroemer, G., and Reed, J. C. (2000) *Nat. Med.* **6**, 513–519
24. Wang, X. (2001) *Genes Dev.* **15**, 2922–2933
25. Larochette, N., Decaudin, D., Jacotot, E., Brenner, C., Marzo, I., Susin, S. A., Zamzami, N., Xie, Z., Reed, J., and Kroemer, G. (1999) *Exp. Cell Res.* **249**, 413–421
26. Blackburn, E. H. (2000) *Nature* **408**, 53–56
27. Chin, L., Artandi, S. E., Shen, Q., Tam, A., Lee, S. L., Gottlieb, G. J., Greider, C. W., and DePinho, R. A. (1999) *Cell* **97**, 527–538
28. Oulton, R., and Harrington, L. (2000) *Curr. Opin. Oncol.* **12**, 74–81
29. Gonzalez-Suarez, E., Samper, E., Flores, J. M., and Blasco, M. A. (2000) *Nat. Genet.* **26**, 114–117
30. Lee, T. C., Wei, M. L., Chang, W. J., Ho, I. C., Lo, J. F., Jan, K. Y., and Huang, H. (1989) *In Vitro Cell. Dev. Biol.* **25**, 442–448
31. Lee, T. C., and Ho, I. C. (1994) *Environ. Health Perspect.* **102**, Suppl. 3, 101–105
32. Kipling, D., and Cooke, H. J. (1990) *Nature* **347**, 400–402
33. Harley, C. B., Futcher, A. B., and Greider, C. W. (1990) *Nature* **345**, 458–460
34. Zijlmans, J. M., Martens, U. M., Poon, S. S., Raap, A. K., Tanke, H. J., Ward, R. K., and Lansdorp, P. M. (1997) *Proc. Natl. Acad. Sci. U. S. A.* **94**, 7423–7428
35. Kipling, D. (1997) *Hum. Mol. Genet.* **6**, 1999–2004
36. Blasco, M. A., Lee, H. W., Hande, M. P., Samper, E., Lansdorp, P. M., DePinho, R. A., and Greider, C. W. (1997) *Cell* **91**, 25–34
37. Lee, H. W., Blasco, M. A., Gottlieb, G. J., Horner, J. W., 2nd, Greider, C. W., and DePinho, R. A. (1998) *Nature* **392**, 569–574
38. Herrera, E., Samper, E., Martin-Caballero, J., Flores, J. M., Lee, H. W., and Blasco, M. A. (1999) *EMBO J.* **18**, 2950–2960
39. Herrera, E., Samper, E., and Blasco, M. A. (1999) *EMBO J.* **18**, 1172–1181
40. Rudolph, K. L., Chang, S., Lee, H. W., Blasco, M., Gottlieb, G. J., Greider, C., and DePinho, R. A. (1999) *Cell* **96**, 701–712
41. Liu, L., Trimarchi, J., Smith, P. J. S., and Keefe, D. (2002) *Aging Cell* **1**, 40–46
42. Liu, L., Blasco, M. A., Trimarchi, J. R., and Keefe, D. L. (2002) *Dev. Biol.* **249**, 74–84
43. Eskes, R., Antonsson, B., Osen-Sand, A., Montessuit, S., Richter, C., Sadoul, R., Mazzei, G., Nichols, A., and Martinou, J. C. (1998) *J. Cell Biol.* **143**, 217–224
44. Hemann, M. T., Strong, M. A., Hao, L. Y., and Greider, C. W. (2001) *Cell* **107**, 67–77
45. Samper, E., Flores, J. M., and Blasco, M. A. (2001) *EMBO Rep.* **2**, 800–807
46. Zhang, X., Mar, V., Zhou, W., Harrington, L., and Robinson, M. O. (1999) *Genes Dev.* **13**, 2388–2399
47. Herbert, B., Pitts, A. E., Baker, S. I., Hamilton, S. E., Wright, W. E., Shay, J. W., and Corey, D. R. (1999) *Proc. Natl. Acad. Sci. U. S. A.* **96**, 14276–14281
48. Mitchell, J. R., and Collins, K. (2000) *Mol. Cell* **6**, 361–371
49. von Zglinicki, T., Saretzki, G., Docke, W., and Lotze, C. (1995) *Exp. Cell Res.* **220**, 186–193
50. Saretzki, G., Sitte, N., Merkel, U., Wurm, R. E., and von Zglinicki, T. (1999) *Oncogene* **18**, 5148–5158
51. Hahn, W. C., Counter, C. M., Lundberg, A. S., Beijersbergen, R. L., Brooks, M. W., and Weinberg, R. A. (1999) *Nature* **400**, 464–468
52. Mathon, N. F., and Lloyd, A. C. (2001) *Nat. Rev. Cancer* **1**, 203–213
53. Hackett, J. A., and Greider, C. W. (2002) *Oncogene* **21**, 619–626
54. Cotgreave, I. A. (1997) *Adv. Pharmacol.* **38**, 205–227
55. Mayer, M., and Noble, M. (1994) *Proc. Natl. Acad. Sci. U. S. A.* **91**, 7496–7500
56. Mirkes, P. E., and Little, S. A. (2000) *Toxicol. Appl. Pharmacol.* **162**, 197–206
57. Waxman, S., and Anderson, K. C. (2001) *Oncologist* **6**, 3–10